Twisted photons and electrons

as a new tool

in atomic and nuclear physics

Valeriy G. SERBO

Novosibirsk State University, Novosibirsk, Russia

Plan:

1. Introduction

2. Twisted photons

3. Compton scattering of twisted photons

4. Absorption of twisted light by hydrogen-like atoms

5. Photoionization and radiative recombination with twisted photons and electrons

6. Scattering of twisted electrons on atoms in the Born approximation

7. Conclusion

This report is based mainly on our recent papers:

[1] U.D. Jentschura, V.G. Serbo "Generation of High–Energy Photons with Large Orbital Angular Momentum by Compton Backscattering", Phys. Rev. Lett. 106 (2011) 013001

[2] U.D. Jentschura, V.G. Serbo "Compton Upconversion of Twisted Photons: Backscattering of Particles with Non-Planar Wave Functions", Eur. Phys. Journ. C 71 (2011) 1571

[3] I.P. Ivanov, V.G. Serbo "Scattering of twisted particles: extension to wave packets and orbital helicity", Phys. Rev. A 84 (2011) 033804

[4] O. Matula, A.G. Hayrapetyan, V.G. Serbo, A. Surzhykov, S. Fritzsche. “Atomic ionization of hydrogen-like ions by twisted photons: angular distribution of emitted electrons”,
Journal of Physics B 46 (2013) 205002

[5] O. Matula, A.G. Hayrapetyan, V.G. Serbo, A. Surzhykov, S. Fritzsche. “Radiative capture of twisted electrons by bare ions”,
New Journal of Physics 16 (2014) 053024

[6] H. M. Scholz-Marggraf, S. Fritzsche, V. G. Serbo, A. Afanasev, A. Surzhykov. “Absorption of twisted light by hydrogenlike atoms”.
Physical Review A 90 (2014) 013425

[7] G.L. Kotkin, V.G. Serbo, A. Surzhykov. “Scattering of twisted electrons on atoms in the Born approximation”. In preparation

1. Introduction

There are **two** well-known types of photon waves: plane waves and spherical waves.

The plane wave is the stationary state with a defined energy ω, momentum $\mathbf{k}$ and helicity Λ. **Realization $\rightarrow$ laser flashes.**

The spherical wave is the stationary state with a defined energy ω, total angular momentum J, projection of the total angular momentum $J_z = M$ and parity P. **Realization $\rightarrow$ atomic or nuclear transitions.**

(here and below $\hbar = 1$ and $c = 1$)

What is not so well-known is the fact that there is also **cylindrical waves also known as Bessel waves.**

The Bessel wave is the stationary state with a defined energy ω, longitudinal momentum k_z, projection of the total angular momentum $J_z = M$ and helicity Λ.

Certainly, such state should have non-zero ORBITAL ANGULAR MOMENTUM (OAM).

Usually, these states of photons are called

“TWISTED PHOTONS”.

An interesting research direction in modern optics (last twenty years) is closely related to the experiments with such twisted photons.

These are states of the laser beam whose photons have a non-zero value m **of the ORBITAL ANGULAR MOMENTUM PROJECTION** on the beam propagation axis where m is a (large) integer

L. Allen et al., Phys. Rev. A 45, 8185 (1992);

S. Franke-Arnold, L. Allen, M. Padgett, Laser and Photonics Reviews 2, 299 (2008);

A.M. Yao, M.J. Padgett, Advances in Optics and Photonics 3, 161 (2011).

An experimental realization exists for states with projections as large as $m = 200$

J. E. Curtis, B. A. Koss, and D. G. Gries, Opt. Commun. **207**, 169 (2002).

The wavefront of such states **rotates around the propagation axis**, and their Poynting vector looks like **a corkscrew**:

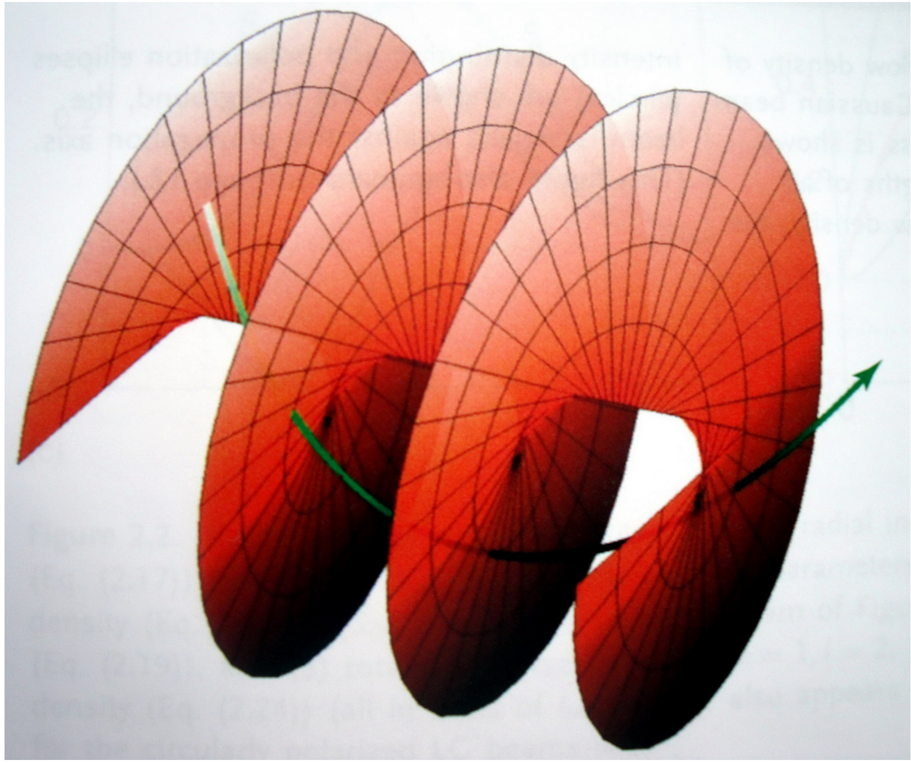

Such photons can be created, for example, from usual laser beams using **spiral phase plate:**

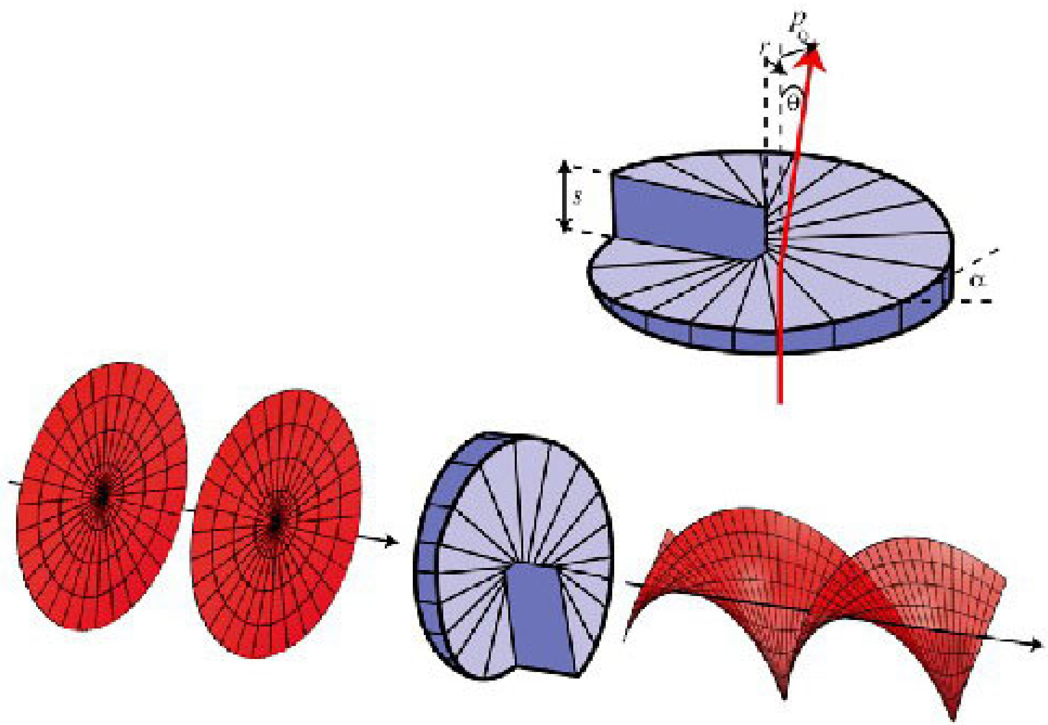

A spiral phase plate can generate a helically phased beam from a Gaussian. In this case $\ell = 0 \rightarrow \ell = 2$.

or a **numerically computed hologram:**

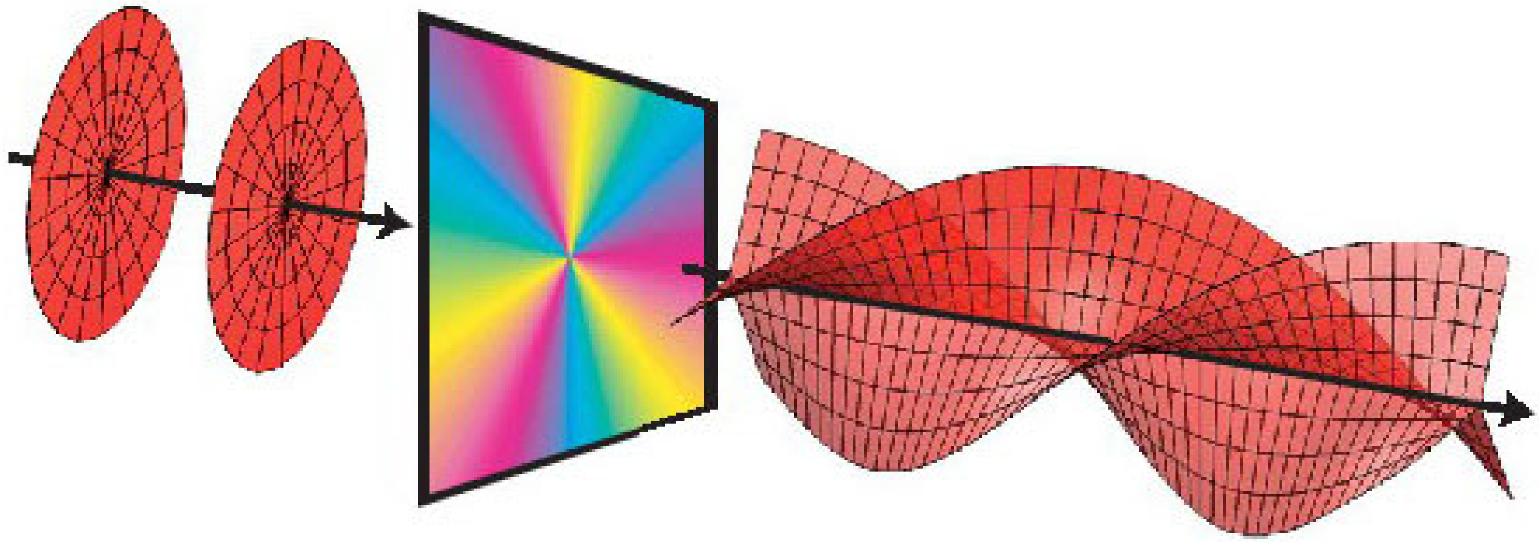

A helical phase profile $\exp(i\ell\phi)$ converts a Gaussian laser beam into a helical mode whose wave fronts resemble an ℓ-fold corkscrew. In this case $\ell = 3$.

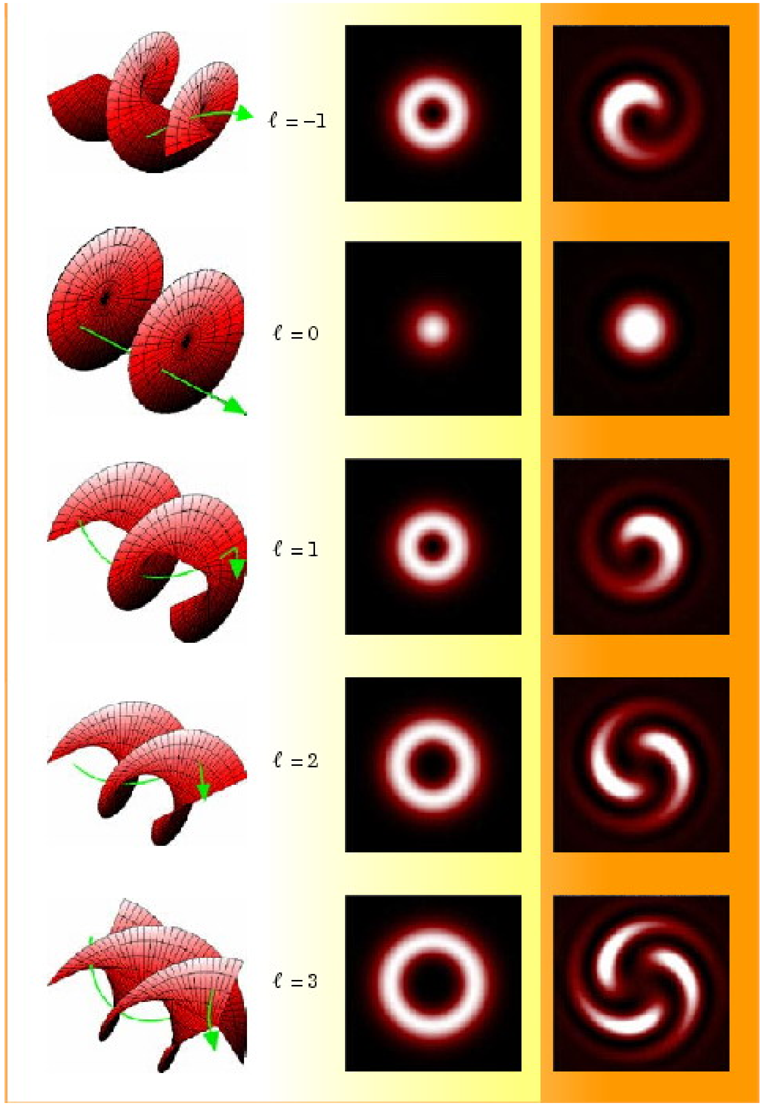

$\ell = -1$
$\ell = 0$
$\ell = 1$
$\ell = 2$
$\ell = 3$

Some examples of applications of such photons:

See a new book

Twisted photons

(Applications of light with orbital angular momentum)

edd. by J. P. Torres and L. Torner

(Wiley-VCH Weinheim, Germany 2011)

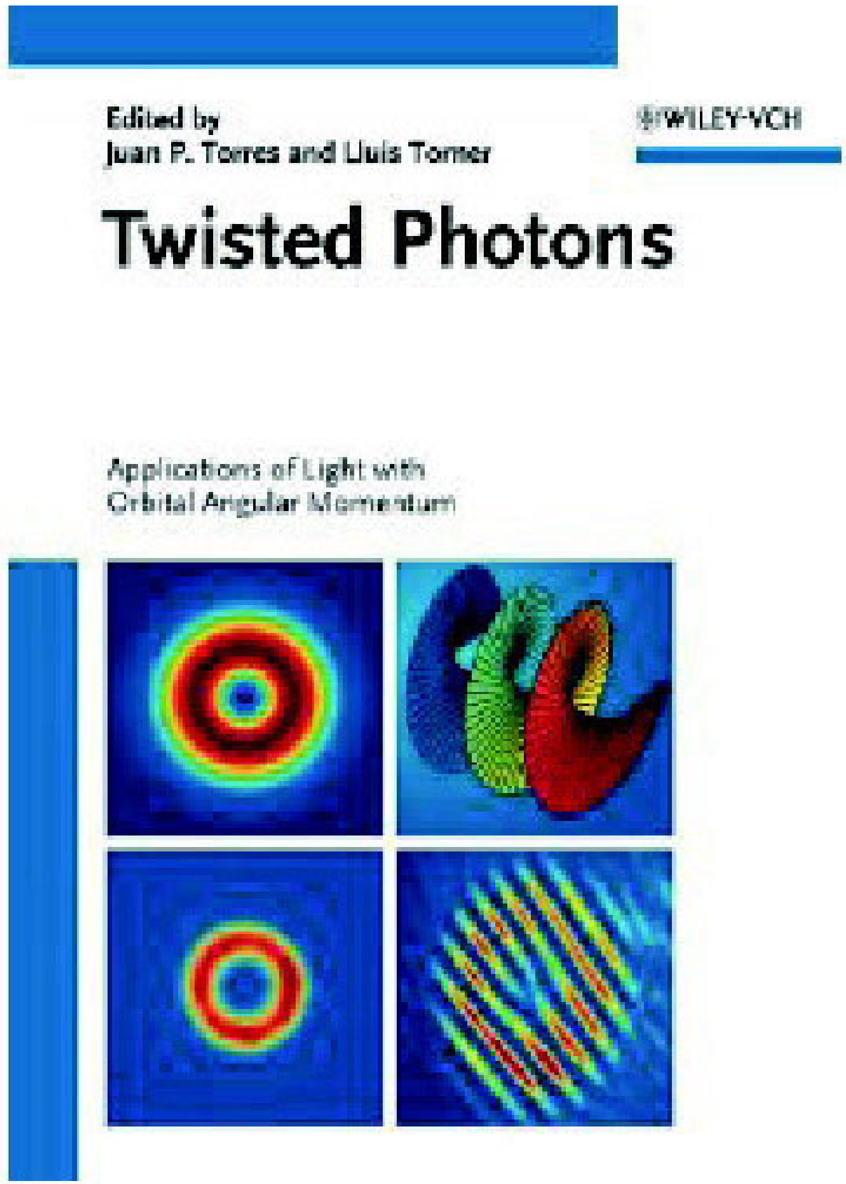
Edited by
Juan P. Torres and Lluis Torner
WILEY-VCH
Twisted Photons
Applications of Light with
Orbital Angular Momentum

[1.] Micro-machines — it was demonstrated that micron-sized Teflon and calcite “particles” start to rotate after absorbing twisted photons

[2.] Astrophysics — the observation of orbital angular momentum of light scattered by rotating black holes could be very instructive

[3.] Rotating atoms with light — rotating Bose-Einstein condensates

[4.] Spiral phase contrast microscopy

[5.] Optical torques in liquid crystals

[6.] Quantum information — quantum features in high-dimensional Hilbert spaces

Very recently several groups have reported successful creation of **twisted electrons**, first using phase plates
M. Uchida and A. Tonomura, Nature **464**, 737 (2010)

and then with computer-generated holograms
J. Verbeeck, H. Tian, P. Schlattschneider, Nature **467**, 301 (2010); B. J. McMorran et al, Science **331**, 192 (2011)

Such electrons carried the energy as high as 300 keV and the orbital quantum number up to $m = 75$.

It is very conceivable that when these electrons are injected into a linear electron accelerator, their energy can be boosted into the multi-MeV and even GeV region.

Such vortex beams can be manipulated and focused just as the usual electron beams, and very recently **remarkable focusing of a vortex electron beam** to the focal spot of

less than $1.2 \cdot 10^{-8}$ cm = 0.12 nm in diameter

was achieved — see the paper:

"Atomic scale electron vortices for nanoresearch"

Verbeeck, Schattschneider, Lazar, Stöger-Pollach, Löffler, Steiger-Thirsfeld, Van Tendeloo, Appl. Phys. Lett. **99**, 203109 (2011)

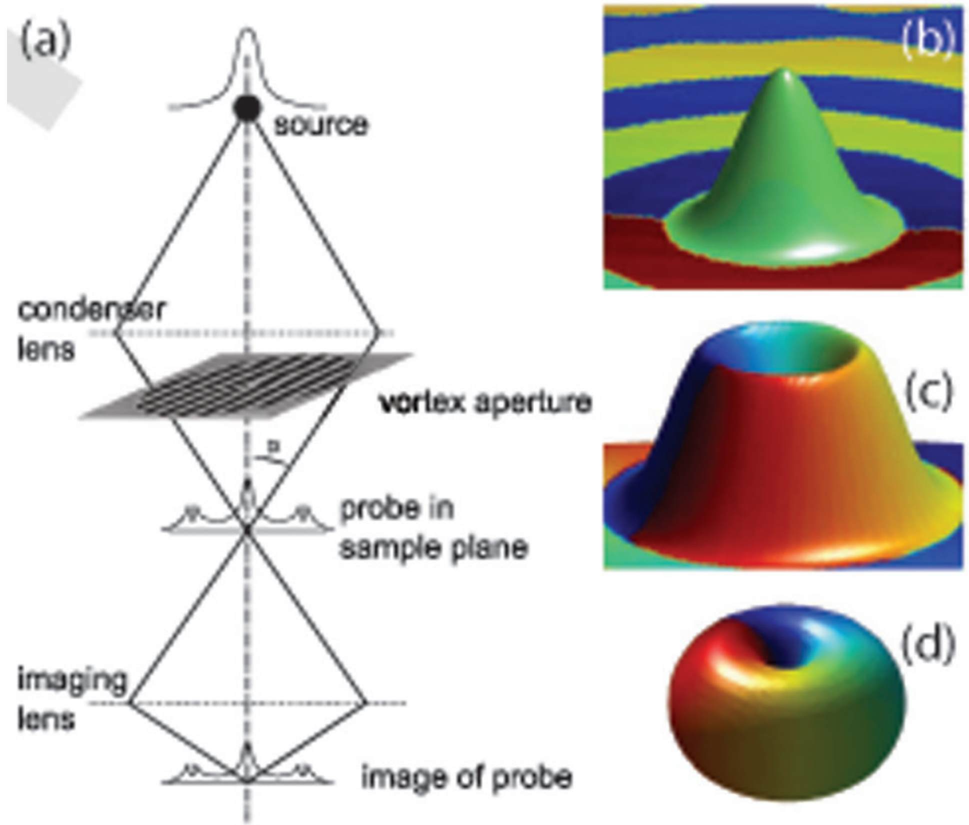

FIG. 1. (Color online) (a) Sketch of the setup to create focused vortex probes in a transmission electron microscope. The probe is formed in the sample plane and can be used to perform atomic resolution experiments in that plane. The probe is magnified for observation by the imaging system. The convergence angle α can be adjusted which allows to tune the size of the vortex. (b), (c) Artist impression of the intensity distribution for a conventional airy disc and a vortex beam with the same opening angle. (d) Sketch of the surface of a $2p_1$ orbital in nitrogen containing 80% of the electron density. The image is approximately to scale with (b), (c) for our experimental setting of $\alpha = 21.4$ mrad. Color coding indicates the phase distribution from 0 (blue) to 2π (red). Note the big similarity in both phase

In the papers [1–3] we have shown that it is possible to convert twisted photons from an energy range of about 1 eV to a higher energies of up to several GeV using Compton backscattering off ultra-relativistic electrons.

In principle, Compton backscattering is **an established method** for the creation of high-energy photons and is used successfully in various application areas:

For example, in Novosibirsk Budker INP on the ROKK-2M device with the electron energy 5 GeV, **final backscattered photons with the energy up to 0.5 GeV** were produced for the study of **photo-nuclear reactions** and for NQED experiments including of **the photon splitting and the Delbrück scattering**.

However, the central question is how to treat Compton backscattering of twisted photons whose field configuration is significantly different from plane waves.

2. Twisted photons

Twisted scalar particle

The usual plane-wave state of a scalar particle with mass equals to zero has a defined 3-momentum $\boldsymbol{k}$, energy $\omega = |\boldsymbol{k}|$, and its wave function reads

$$\Psi_{\boldsymbol{k}}(t, \boldsymbol{r}) = \mathrm{e}^{-\mathrm{i}(\omega t - \boldsymbol{k}\boldsymbol{r})}\,. \qquad (1)$$

A twisted scalar particle has the following quantum numbers:
longitudinal momentum k_z,
absolute value of the transverse momentum $\varkappa$,
energy $\omega = |\boldsymbol{k}| = \sqrt{\varkappa^2 + k_z^2}$
and projection m of the **orbital angular momentum** onto the z axis:

$$\partial_\mu \partial^\mu \, \Psi_{\varkappa m k_z}(t, \boldsymbol{r}) = 0\,, \tag{2}$$

$$\check{p}_z \, \Psi_{\varkappa m k_z} = k_z \, \Psi_{\varkappa m k_z}\,, \;\; \check{p}_z = -\mathrm{i}\frac{\partial}{\partial z}, \tag{3}$$

$$\check{L}_z \, \Psi_{\varkappa m k_z} = m \, \Psi_{\varkappa m k_z}\,, \quad \check{L}_z = -\mathrm{i}\frac{\partial}{\partial \varphi_r}\,. \tag{4}$$

The evident form of the corresponding wave function in cylindrical coordinates $r_\perp$, φ_r, z is

$$\Psi_{\varkappa m k_z}(r_\perp, \varphi_r, z, t) = \mathrm{e}^{-\mathrm{i}(\omega t - k_z z)}\, \psi_{\varkappa m}(r_\perp, \varphi_r)\,,$$

$$\psi_{\varkappa m}(r_\perp, \varphi_r) = \frac{\mathrm{e}^{\mathrm{i} m \varphi_r}}{\sqrt{2\pi}}\, \sqrt{\varkappa}\, J_m(\varkappa\, r_\perp)\,, \qquad (5)$$

where $J_m(x)$ is **the Bessel function**.

For small $r_\perp \ll 1/\varkappa$, the function $\psi_{\varkappa m}(r_\perp, \varphi_r)$ is of order of $r_\perp^m$, has a maximum at $r_\perp \sim m/\varkappa$, and then drops at large values $r_\perp \gg 1/\varkappa$

$$\psi_{\varkappa m}(r_\perp, \varphi_r) \approx \frac{\mathrm{e}^{\mathrm{i} m \varphi_r}}{\pi \sqrt{r}}\, \cos\left(\varkappa\, r_\perp - \frac{m\,\pi}{2} - \frac{\pi}{4}\right). \qquad (6)$$

The function $\psi_{\varkappa m}(r_\perp, \varphi)$ may be expressed as a **superposition of plane waves** in the xy plane,

$$\psi_{\varkappa m}(r_\perp, \varphi) = \int a_{\varkappa m}(\boldsymbol{k}_\perp)\, \mathrm{e}^{\mathrm{i}\boldsymbol{k}_\perp \boldsymbol{r}_\perp} \frac{\mathrm{d}^2 k_\perp}{(2\pi)^2}, \tag{7}$$

where the Fourier amplitude $a_{\varkappa m}(\boldsymbol{k}_\perp)$ is concentrated on the circle with $k_\perp \equiv |\boldsymbol{k}_\perp| = \varkappa$,

$$a_{\varkappa m}(\boldsymbol{k}_\perp) = (-\mathrm{i})^m\, \mathrm{e}^{\mathrm{i}m\varphi_k} \sqrt{\frac{2\pi}{k_\perp}}\, \delta(k_\perp - \varkappa)\,. \tag{8}$$

Therefore, the function $\Psi_{\varkappa m k_z}(r_\perp, \varphi_r, z, t)$ can be regarded as a superposition of the plane waves with the defined longitudinal momentum k_z, absolute value of transverse momentum $\varkappa$, energy $\omega = \sqrt{\varkappa^2 + k_z^2}$ and different directions of the vector $\boldsymbol{k}_\perp$ given by the angle φ_k.

Using such type of the state, we have considered in papers [5] and [7] the radiative recombination of twisted electrons on bare ions and the elastic scattering of the fast but non-relativistic twisted electrons on atoms in the Born approximation.

The first results appear very unusual, yet quite interesting!

Twisted photons

The wave function of a twisted photon (vector particle) can be constructed as a generalization of the scalar wave function. We start from the plane-wave photon state with **a defined 4-momentum** $k = (\omega, \boldsymbol{k})$ and **helicity** $\Lambda = \pm 1$,

$$A^{\mu}_{k\Lambda}(t, \boldsymbol{r}) = e^{\mu}_{k\Lambda}\, \mathrm{e}^{-\mathrm{i}(\omega\, t - \boldsymbol{k}\boldsymbol{r})} \tag{9a}$$

$$e_{k\Lambda} \cdot k = 0\,, \quad e^{*}_{k\Lambda} \cdot e_{k\Lambda'} = -\delta_{\Lambda\Lambda'}\,, \tag{9b}$$

where $e^{\mu}_{k\Lambda}$ is the polarization four-vector of the photon.

The twisted photon vector potential

$$\mathcal{A}^{\mu}_{\varkappa m k_z \Lambda}(r, \varphi_r, z, t) = \int a_{\varkappa m}(\boldsymbol{k}_\perp)\, A^{\mu}_{k\Lambda}(t, \boldsymbol{r})\, \frac{\mathrm{d}^2 k_\perp}{(2\pi)^2} \tag{10}$$

$$= (-\mathrm{i})^m \sqrt{2\pi\varkappa} \int_0^{2\pi} \mathrm{d}\varphi_k \int_0^{\infty} \mathrm{d}k_\perp\, \delta(k_\perp - \varkappa)\, \frac{e^{\mathrm{i}m\varphi_k}}{(2\pi)^2}\, A^{\mu}_{k\Lambda}(t, \boldsymbol{r})$$

is given as a two-fold integral over the perpendicular components $\boldsymbol{k}_\perp = (k_x, k_y, 0)$ of the wave vector $\boldsymbol{k} = (k_x,\, k_y,\, k_z)$.

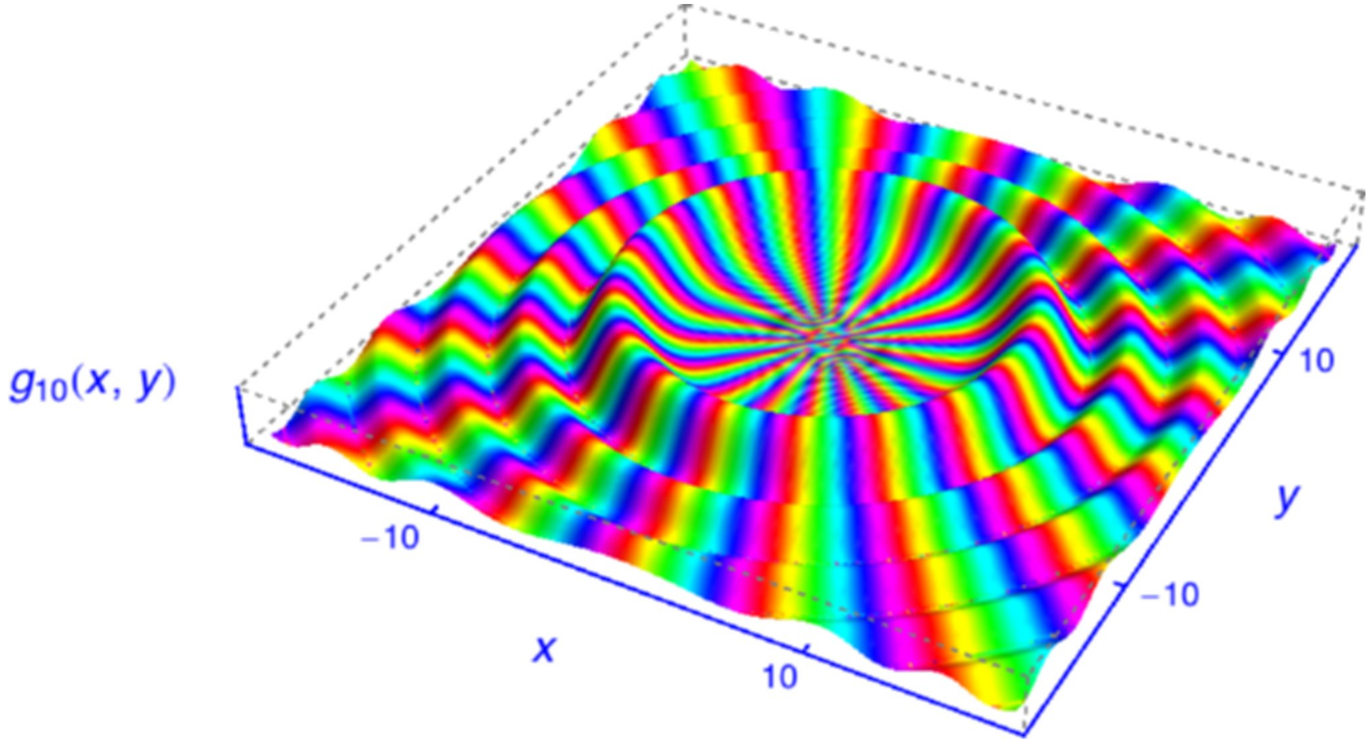

The vector potential $\mathcal{A}^{\mu}_{\varkappa m k_z \Lambda}$ of the twisted photon is presented as $g_m(x, y) = |\mathcal{A}^{\mu}_{\varkappa m k_z \Lambda}(0, x, y, 0)|^2$, which is a function of x and y. The parameters are $\mu = 1$ (x component), $m = 10$, $\varkappa = 1$.

Detailed description of this state is given in our paper [4]

The function $\mathcal{A}^{\mu}_{\varkappa m k_z \Lambda}(r, \varphi_r, z, t)$ can be regarded as a superposition of **plane waves**
with defined longitudinal momentum k_z, absolute value of transverse momentum $\varkappa$, energy $\omega = \sqrt{\varkappa^2 + k_z^2}$, helicity Λ and different directions of the vector $\boldsymbol{k}_\perp$ given by the angle φ_k.

This stationary state has also a defined z-projection of the total angular momentum $J_z = L_z + S_z = m$ while $L_z = m,\ m \pm 1$.

In papers [4] and [6] we use such type of photon states for the study
the photo-excitation and photo-ionization of the hydrogen atom.

3. Compton scattering of twisted photons

3.1. Compton scattering of plane-wave photons

The S-matrix element for plane waves is well known

$$S_{fi}^{(\mathrm{PW})} = \mathrm{i}\,(2\pi)^4\,\delta^{(4)}(p + k - p' - k')\,\frac{M_{fi}}{4\sqrt{E\,E'\,\omega\,\omega'}}\,, \qquad (11)$$

where M_{fi} is the amplitude.

For **a head-on collision of a plane-wave laser photon and ultra-relativistic electron**, **the final photon propagates almost in the same direction as the momentum of the initial electron with the typical scattering angles** $\sim 1/\gamma_e$.

3.2. Compton scattering with the twisted photon in the initial state

Since the twisted photon is a superposition of plane-wave photons, for the case where the **initial photon is twisted** m-photon, but the **outgoing one is a plane-wave** photon, we have

$$S_{fi}^{(\mathrm{m})} \equiv \langle k', \Lambda'; p', \lambda' | S | \varkappa, m, k_z, \Lambda; p, \lambda \rangle$$
$$= \int \frac{\mathrm{d}^2 k_\perp}{(2\pi)^2} S_{fi}^{(\mathrm{PW})} \, a_{\varkappa m}(\boldsymbol{k}_\perp) \,. \quad (12)$$

A detailed consideration shows that the corresponding cross section is given by the standard expression with the only replacement being

$$x = \frac{4\omega E}{m_e^2} \to \frac{4\omega E}{m_e^2} \cdot \cos^2(\theta_k/2) \,, \quad (13)$$

where θ_k is the conical angle of the initial photon $\tan\theta_k = k_\perp/|k_z|$.

This is important since it proves that the cross section for the

twisted initial photons has no additional smallness

as compare with the ordinary Compton scattering.

This result looks very natural since the initial photon state is nothing else but **a superposition of plane waves with the same absolute value of their transverse momentums**.

3.3. Compton scattering for twisted photons in the initial and final states

Strict BACKWARD scattering and PRINCIPAL conclusion

For strict backward Compton scattering the transverse momentum of the **final electron** is $\mathbf{p}'_\perp = 0$.

Therefore, the **final twisted** m' photon is a superposition of plane waves with
large energy $\omega' \sim 4\gamma^2\omega$
and **small transverse momentum** $\boldsymbol{k}'_\perp = \boldsymbol{k}_\perp$:

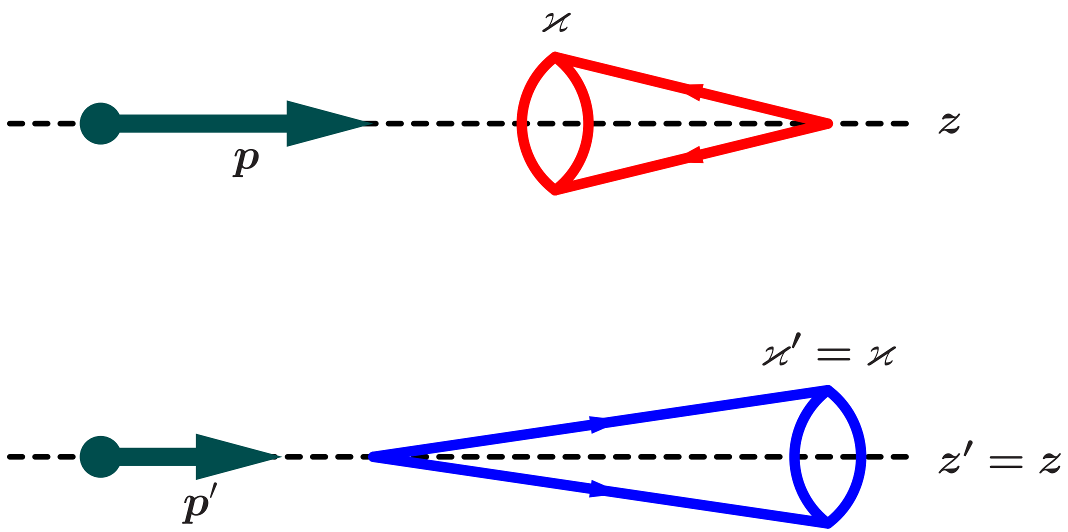

Fig. 4. Initial (above) and final (below) states for the head-on Compton **strick-backscattering** geometry of the twisted photons

The S matrix element $S_{fi}^{(\mathrm{TW})}$ for the scattering of the twisted (TW) photon $|\varkappa, m, k_z, \Lambda\rangle$ into the state $|\varkappa', m', k'_z, \Lambda'\rangle$ is given as a convolution:

$$S_{fi}^{(\mathrm{TW})} = \int \frac{\mathrm{d}^2 k_\perp}{(2\pi)^2} \frac{\mathrm{d}^2 k'_\perp}{(2\pi)^2} \, a^*_{\varkappa' m'}(\boldsymbol{k}'_\perp) \, S_{fi}^{(\mathrm{PW})} \, a_{\varkappa m}(\boldsymbol{k}_\perp) \, . \qquad (14)$$

For strict backscattering, we have found that the angular momentum projection $m' = m$ and the conical momentum spread $\varkappa' = \varkappa$ of the twisted photons **are conserved**, but the energy of the final twisted photon **is increased** dramatically: $\omega'/\omega \sim 4\gamma^2 \gg 1$.

It means that there is a principal possibility to create high-energy photons with large orbital angular momenta projections.

3.4. General case
(orbital helicity; wave pockets for twisted states)

What happens for non-strict backscattering of the twisted photons?

This problem is studied in detail in the paper [3]

In general case the final electron momentum is $\boldsymbol{p}' \nparallel \boldsymbol{p}$, and thus it is natural to consider the final twisted photon as propagating along the axis z' which is the axis of **the average propagation direction** of the final photon. **The corresponding projection of OAM we call ORBITAL HELICITY**

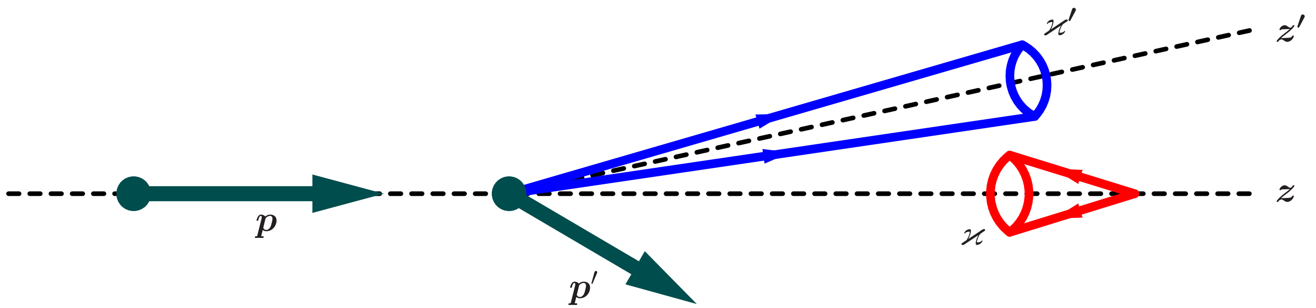

Fig. 6. Initial (red) and final (blue) states of the twisted photons for the head-on Compton **non-strick backscattering** geometry.

We denote the angle between axes z and z' as $\langle\theta_\gamma\rangle$

For this case, we consider **the realistic case** when the pure initial twisted state $\psi_{\varkappa m}(r,\varphi)$ is replaced by **a wave packet** with a defined m:

$$\psi_{\varkappa m}(r,\varphi) \to \psi_m(r,\varphi) = \int_0^\infty f(\varkappa)\psi_{\varkappa m}(r,\varphi)\, d\varkappa$$

with the narrow weight function of the Gaussian type

$$f(\varkappa) = N \exp\left[-\frac{(\varkappa-\varkappa_0)^2}{2\sigma^2}\right], \tag{15}$$

peaking at $\varkappa = \varkappa_0$ and having a width σ.

We assume the similar smearing for the **final** twisted state $\psi_{\varkappa' m'}(r,\varphi)$ with the weight function $g(\varkappa')$.

A further consideration shows that the distribution over the final projection m' is now **concentrated near the initial value m**:

$$|m' - m| \lesssim 4\langle\theta_\gamma\rangle \, \frac{\omega}{\sigma} \, .$$

(Note that the right-hand side of this inequality is **small** for the small enough angles $\langle\theta_\gamma\rangle$).

As a result, we have proven that if the initial and final states are wave packets, then

final orbital helicity m' stays close to m,

and the final $\varkappa'$ stays close to $\varkappa$.

4. Absorption of twisted light by hydrogen-like atoms

In papers

A. Picón et al. Optical Express 18 (2010) 3660

A. Afanasev, C. Carlson, A. Mukheriee. ArXive 1304.0115 and 1305.3650

Ref. [6] H. M. Scholz-Marggraf, S. Fritzsche, V. G. Serbo, A. Afanasev, A. Surzhykov. Phys. Rev. A 90 (2014) 013425

it was considered **the atomic excitation by the twisted photons.** **The authors point out several unique possibilities arising due to non-zero orbital angular momentum of the initial photon.**

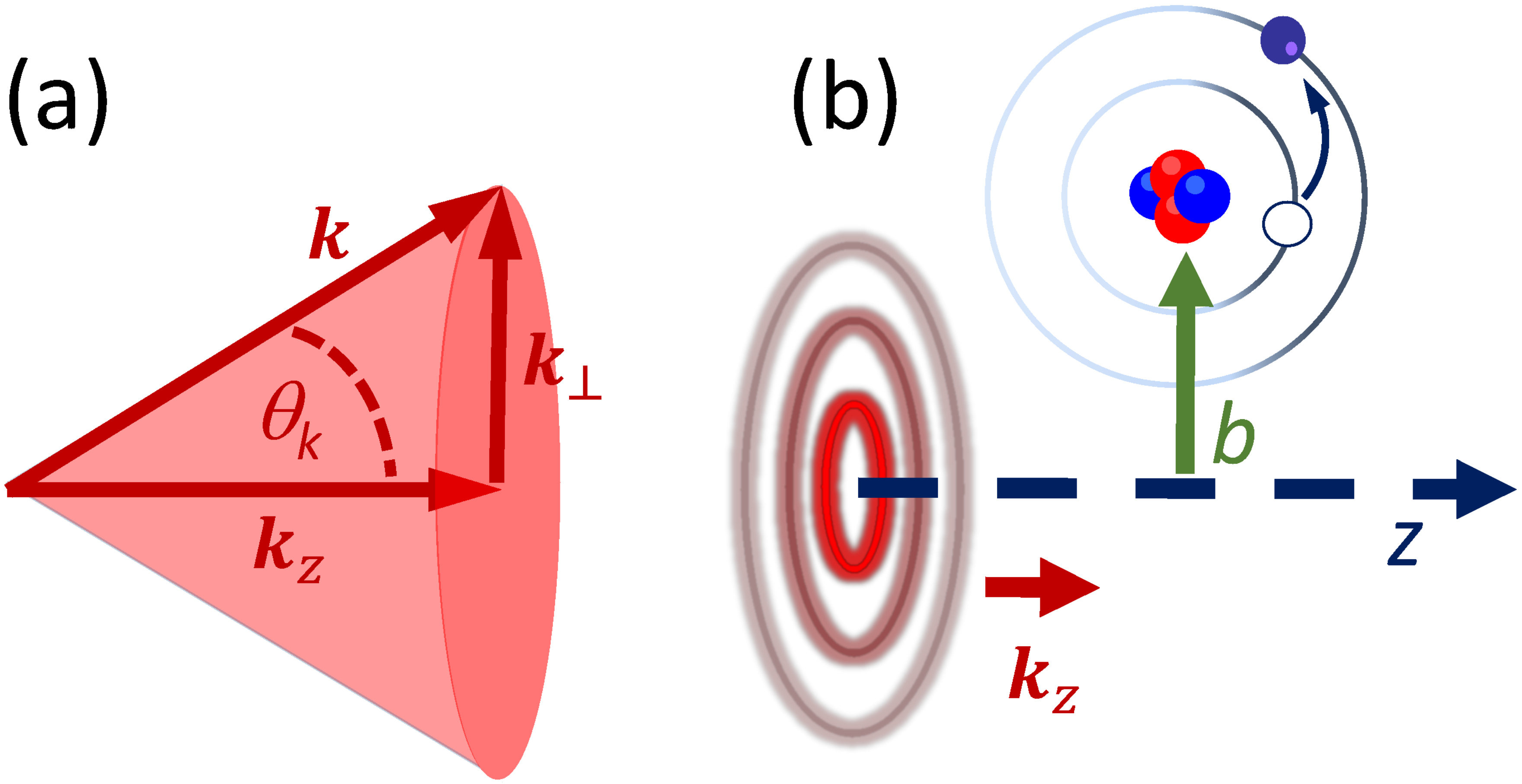
(a)
$\boldsymbol{k}$
$\boldsymbol{k}_{\perp}$
θ_k
$\boldsymbol{k}_z$
(b)
b
z
$\boldsymbol{k}_z$

In particular, the paper [6] presents a theoretical study of the excitation of hydrogenlike atoms by twisted light using the non-relativistic first-order perturbation theory.

In this paper, two scenarios in which **the Bessel beam** collides with either **a well-localized single atom or with randomly distributed atoms** are considered. Detailed calculations have been performed for the second, more experimentally realistic case.

Cross sections for selected transitions are derived and atomic sublevel populations due to the interactions of twisted light with macroscopic assemblies of atoms are analyzed. While these are interesting results, the main contribution here is definitely **the powerful theoretical method for the studies of the twisted particle interactions**.

Calculations performed for the $1s \to 2p$ and $2p \to 3d$ transitions clearly indicate that **sublevel population of excited atoms following absorption of the twisted photons differs much from what is expected for the standard plane–wave case**; an effect that can be easily observed experimentally by measuring the linear polarization of the subsequent fluorescent emission.

In Fig. below we display the θ_k–dependence of the **relative total**:

$$\frac{\sigma^{(\text{tw})}_{\text{tot}}(\theta_k)}{\sigma^{(\text{pl})}_{\text{tot}}} \equiv \frac{\sum\limits_{m_f} \sigma^{(\text{tw})}_{m_f}(\theta_k)}{\sum\limits_{m_f} \sigma^{(\text{pl})}_{m_f}}, \tag{16}$$

as well as **relative partial** cross sections:

$$\frac{\sigma^{(\text{tw})}_{m_f}(\theta_k)}{\sigma^{(\text{tw})}_{\text{tot}}(\theta_k)} \equiv \frac{\sigma^{(\text{tw})}_{m_f}(\theta_k)}{\sum\limits_{m_f} \sigma^{(\text{tw})}_{m_f}(\theta_k)}, \tag{17}$$

calculated for the $1s \to 2p$ excitation of neutral hydrogen by the incident photons with helicity $\lambda = +1$.

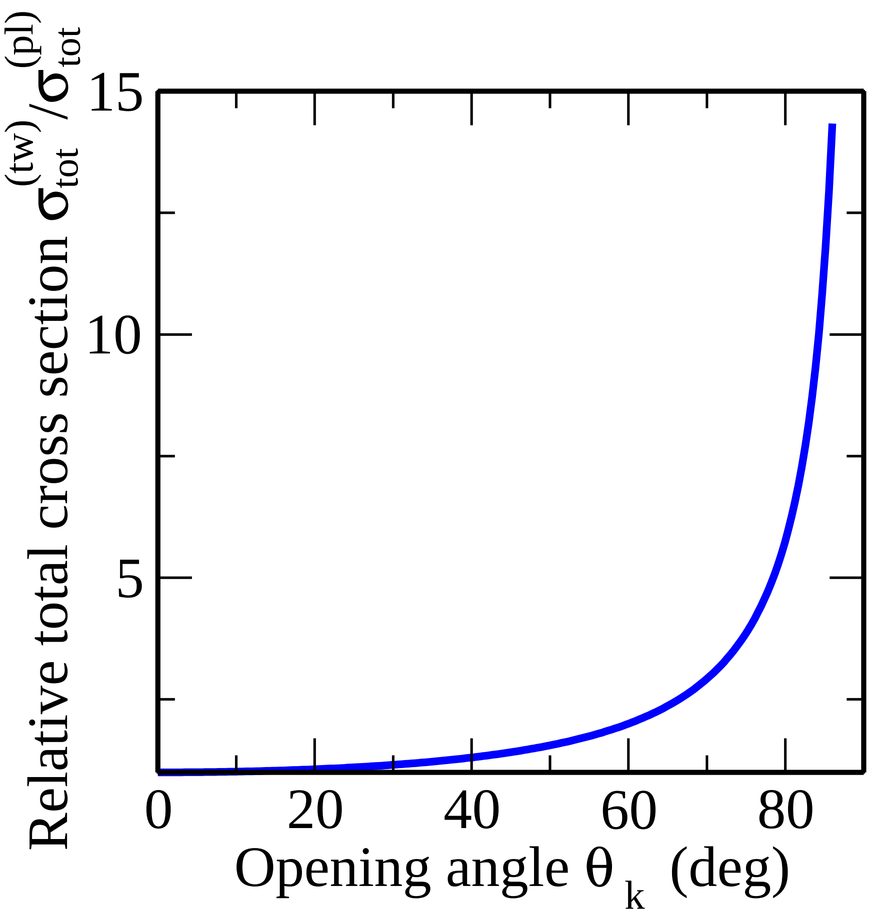
Relative total cross section $\sigma_{tot}^{(tw)}/\sigma_{tot}^{(pl)}$
15
10
5
0
20
40
60
80
Opening angle θ_k (deg)
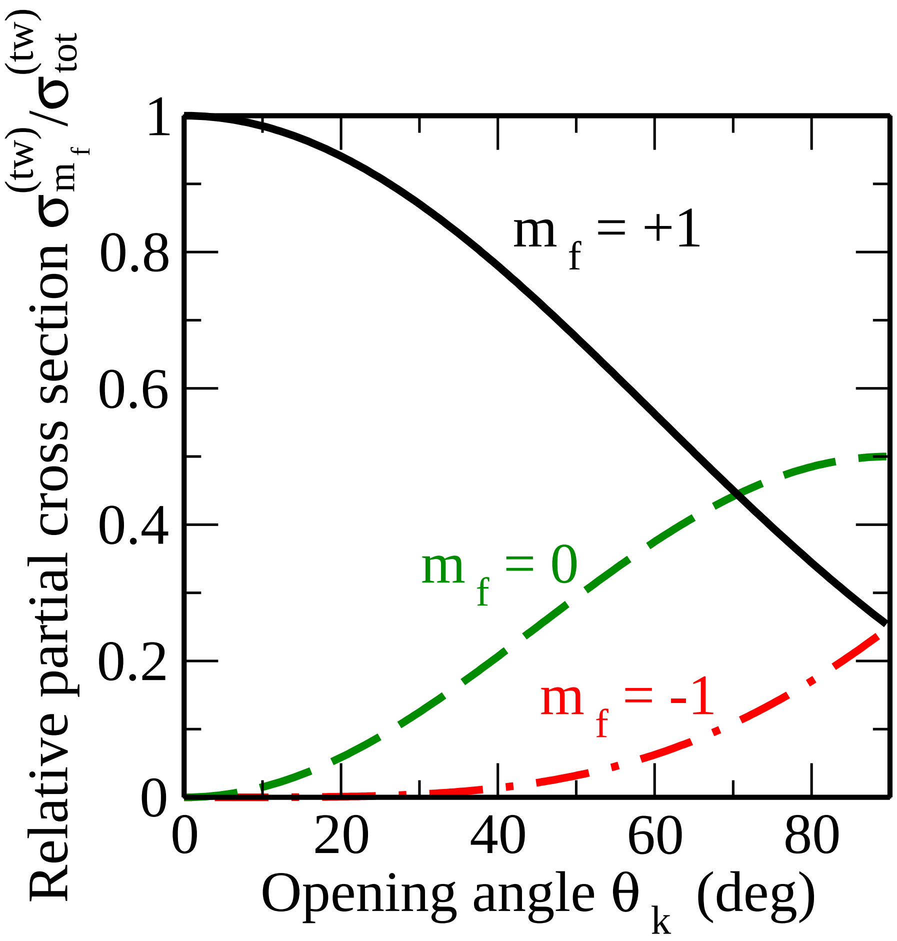
Relative partial cross section $\sigma_{m_f}^{(tw)}/\sigma_{tot}^{(tw)}$
1
0.8
0.6
0.4
0.2
0
20
40
60
80
$m_f = +1$
$m_f = 0$
$m_f = -1$
Opening angle θ_k (deg)

As seen from the above figure, the predictions obtained for the twisted light closely match the "plane–wave" results at vanishing values of the angle θ_k. In particular, only the partial cross section $\sigma^{(\mathrm{tw})}_{m_f=+1}$ is **non–zero** for $\theta_k = 0$, which follows the standard selection rule $m_f = \lambda + m_i = +1$ for $m_i = 0$. Moreover, the $\sigma^{(\mathrm{tw})}_{m_f=+1}(\theta_k = 0)$ coincides with the cross section $\sigma^{(\mathrm{pl})}_{m_f=+1}$, obtained for the incident plane–wave radiation.

With the increase of the transverse momentum $\varkappa$, the absorption of the twisted light **may lead to the population of other substates with $m_f \neq 1$**. As seen from the right panel of the above Fig., for example, the partial cross section for the excitation to the level with $m_f = 0$ grows up with the angle θ_k and even becomes larger than $\sigma^{\mathrm{tw}}_{m_f=+1}(\theta_k)$ for $\theta_k \gtrsim 71^\circ$.

As shown in the above Fig., the partial cross sections $\sigma_{m_f}^{(\mathrm{tw})}(\theta_k)$ for the photo–induced transitions are generally different from each other, thus leading to the **unequal population of the final sublevels** $|n_f\, l_f\, m_f\rangle$. In this case, the excited atom is said to be **aligned and/or oriented**. In atomic theory, such an alignment can be directly employed to analyze the subsequent decay of an atom.

For example, both **the linear polarization and angular distribution** of the Lyman–α ($2p \to 1s$) radiation following the formation of the excited $2p$ state are defined by a **single alignment parameter**:

$$\mathcal{A}_{20} = \frac{1}{2}\,\frac{\sigma_{+1}^{(\mathrm{tw})}(\theta_k) + \sigma_{-1}^{(\mathrm{tw})}(\theta_k) - 2\sigma_{0}^{(\mathrm{tw})}(\theta_k)}{\sigma_{+1}^{(\mathrm{tw})}(\theta_k) + \sigma_{-1}^{(\mathrm{tw})}(\theta_k) + \sigma_{0}^{(\mathrm{tw})}(\theta_k)} = \frac{1}{8}\,(1 + 3\cos 2\theta_k)\;. \quad (18)$$

The information about the θ_k can be experimentally obtained, therefore, from the analysis of the properties of the subsequent Lyman–α decay.

For example, **the linear polarization of the fluorescent photons, detected under the right angle** with respect to the collision (z–) axis, is usually characterized by the Stokes parameter P_1:

$$P_1(\theta_k) = \frac{3\mathcal{A}_{20}(\theta_k)}{\mathcal{A}_{20}(\theta_k) - 6} = \frac{3 + 9\cos 2\theta_k}{-47 + 3\cos 2\theta_k}, \qquad (19)$$

if we assume that the fine structure of the $2p$ level remains unresolved. In experiment, this parameter is determined simply as
$P_1 = (I_{||} - I_{\perp})/(I_{||} + I_{\perp})$,
where $I_{||}$ or $I_{\perp}$ are intensities of light, linearly polarized in parallel or perpendicular directions respectively to the reaction plane.

In Fig. below we display the polarization (19) of the **Lyman–α photons** emitted after the $1s \to 2p$ excitation of neutral hydrogen atoms by the twisted light.

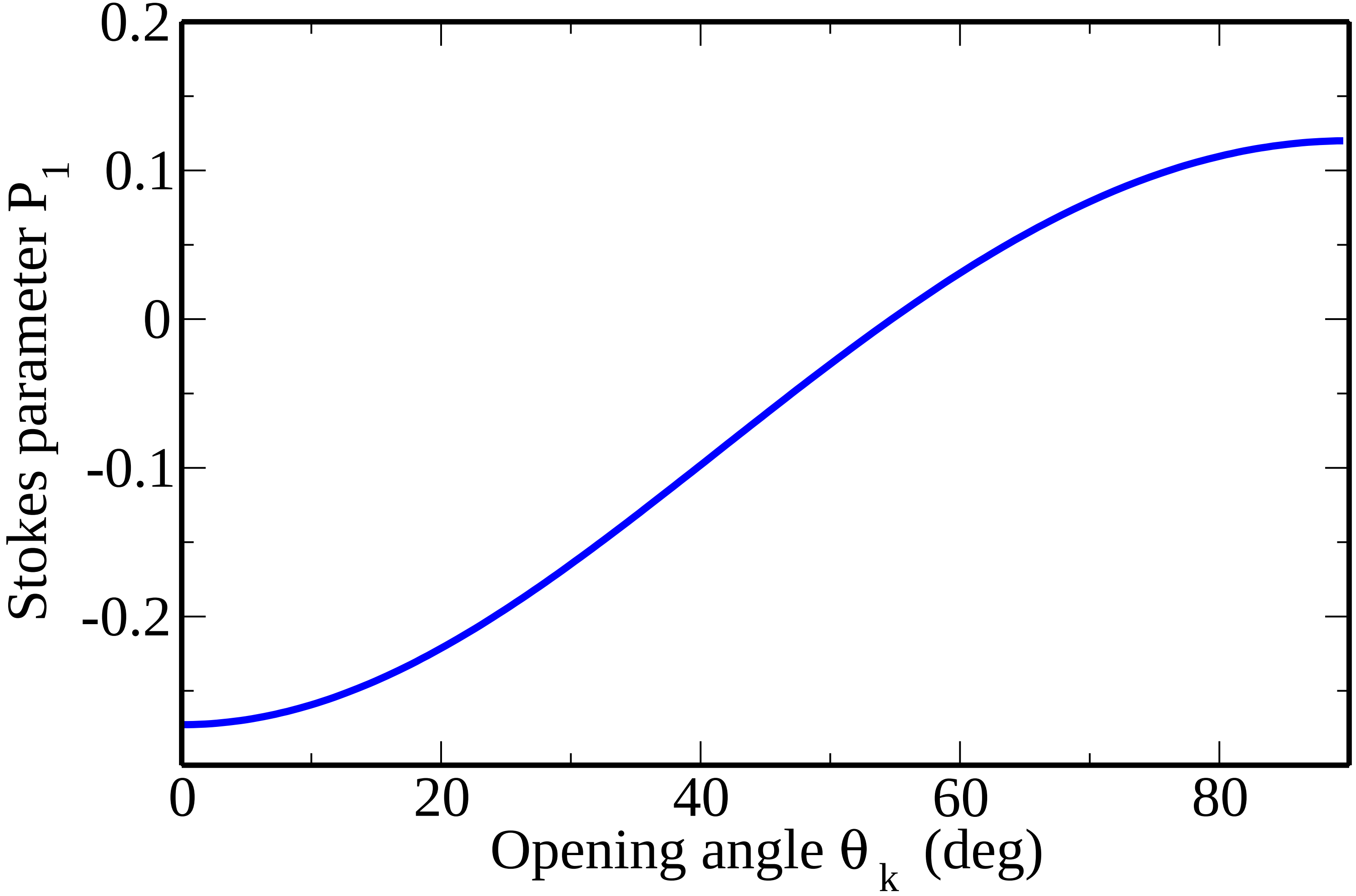
0.2
0.1
0
-0.1
-0.2
Stokes parameter P1
0
20
40
60
80
Opening angle θ k (deg)

Here, one can observe that the parameter $P_1(\theta_k)$ changes **qualitatively** with the opening angle θ_k. Within the paraxial regime where $\theta_k \lesssim 5^\circ$, for example, $P_1(\theta_k)$ is relatively large and **negative**.

With the increase of the opening angle, $P_1(\theta_k)$ first vanishes at $\theta_k \approx 58^\circ$ and later becomes **positive**, which indicates that the fluorescence emission is now predominantly polarized within the plane.

Such a θ_k–variation of the polarization parameter (19) can be easily observed experimentally and may provide valuable information about the interaction of the twisted photon beams with the atomic ensembles.

5. Photoionization and radiative recombination with twisted photons and electrons

In papers

A. Picón et al. Optical Express 18 (2010) 3660

A. Picón et al. New J. Phys. 12 (2010) 083053

it was considered **the atomic photoionization by twisted photons in the paraxial approximation (small θ_k).**

Here we follow our paper

Ref. [4] O. Matula, A.G. Hayrapetyan, V.G. Serbo, A. Surzhykov, S. Fritzsche. J. of Phys. B 46 (2013) 205002 where the **arbitrary** θ_k has been considered. We chose the twisted photon energy as much as **100 eV** (well above the ionization threshold). And we were lucky to find that just a month after our electronic preprint ArXive:1306.3878 had been published, there was an experiment performed by J. Bahrdt, K. Holldack, P. Kuske, R. Müller, M. Scheer, P. Schmid Phys. Rev. Lett. 111 (2013) 034801

In this experiment, the twisted light with **the energy of 99 eV had been produced by utilizing a helical undulator at the synchrotron light source BESSY II**.

Below we present some examples from Ref. [4].

Let us consider **photoionization from the ground state** of hydrogen atom $\psi_{100}(\mathbf{r})$. It is well-known that the corresponding angular distribution of final electrons in the standard case

$$\frac{dW}{d\Omega}(\theta_p, \varphi_p) \propto |\mathbf{e}_{\mathbf{k}\lambda}\mathbf{p}|^2 = \frac{1}{2}\,|p_x + i\lambda p_y|^2 \propto \sin^2\theta_p$$

does not depend on the azimuthal angle φ_p, and it tends to zero at the small polar angle $\theta_p \to 0$. Both these properties are not valid for the twisted light.

First, on the Fig. below we present the results
for $\theta_k \approx \varkappa/k_z = 0.01$ **(the paraxial case)** and
$m_\gamma = +3, \quad \lambda = +1,$
the different impact parameters b
and three polar angles $\theta_p = 45^\circ$ (left panel), $\theta_p = 60^\circ$ (middle panel)
and $\theta_p = 90^\circ$ (right panel) of the electron.

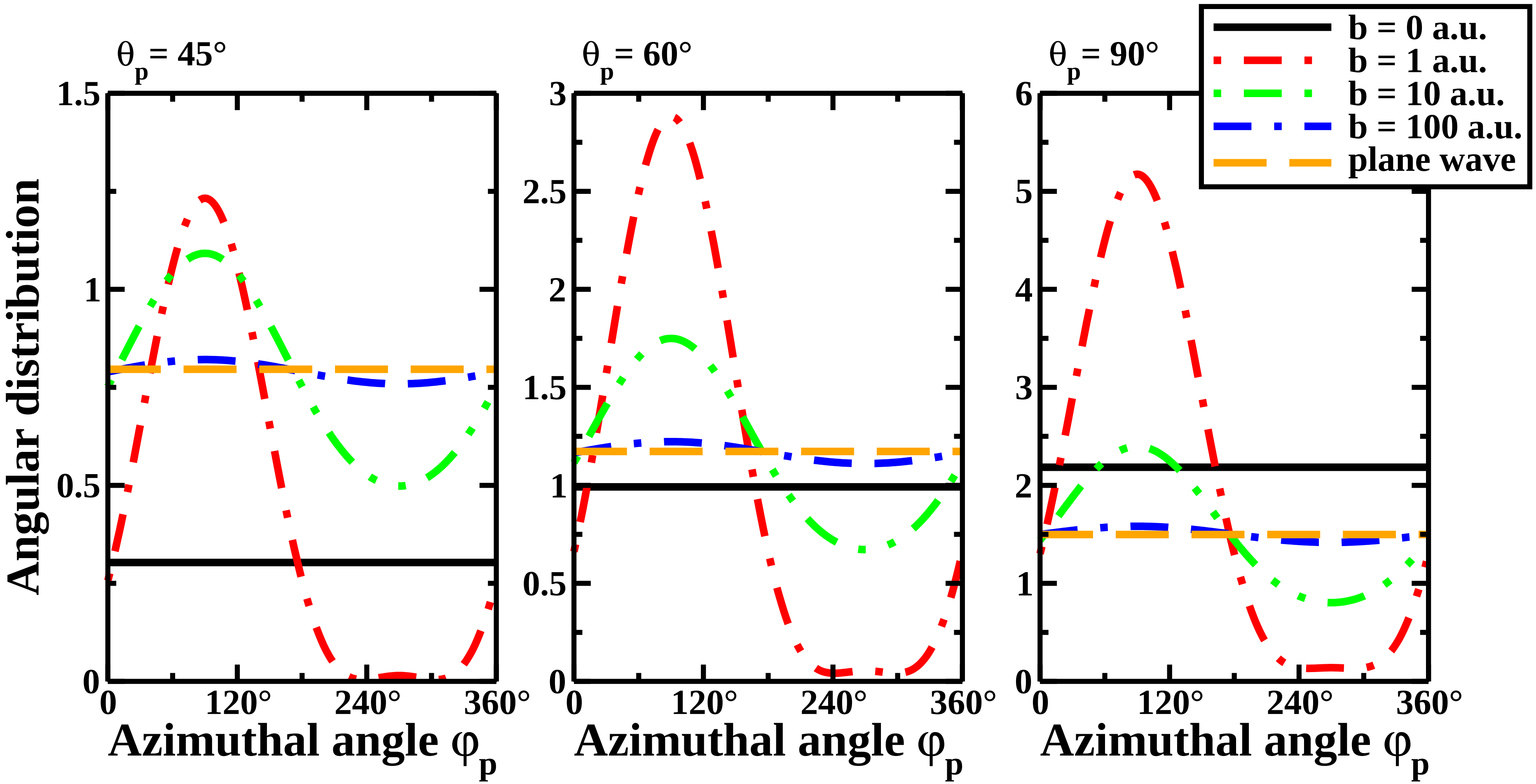

θp = 45°
θp = 60°
θp = 90°
b = 0 a.u.
b = 1 a.u.
b = 10 a.u.
b = 100 a.u.
plane wave
Angular distribution
1.5
1
0.5
0
3
2.5
2
1.5
1
0.5
0
6
5
4
3
2
1
0
0
120°
240°
360°
Azimuthal angle φp

As seen from this Fig., **the angular distribution is isotropic** if the atom is placed in the centre of the wavefront (**at $b = 0$**). This is not unexpected since the system of "atom in the $1s$ state + Bessel beam" possesses for $b = 0$ cylindrical symmetry with respect to the z–axis. **Such a symmetry is broken if the atom position shifts from the zero–intensity centre**. A remarkable anisotropy of the electron emission pattern can be observed, therefore, for impact parameters in the range $0 < b < 100$ a.u. However, if the distance between the atom and the wavefront centre becomes very large, $b > 100$ a.u., the angular distribution converges to the one that results from the plane wave photoionization.

On the next Fig. we present **the same distribution but for the p_y–state of hydrogen atoms** given by the wave function
$\psi_{2,1,+1}(\mathbf{r}) + \psi_{2,1,-1}(\mathbf{r})$

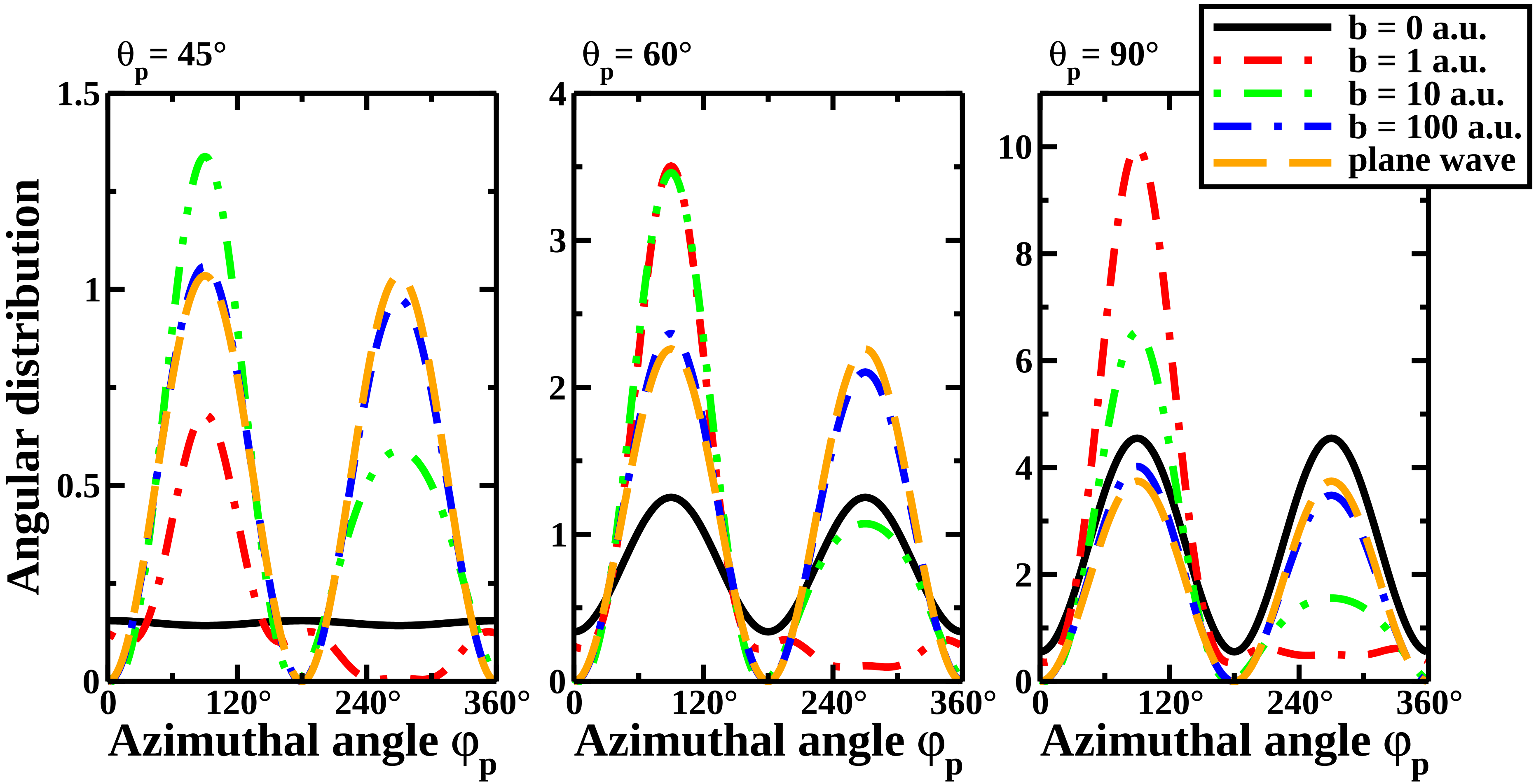

θp = 45°
θp = 60°
θp = 90°
Angular distribution
Azimuthal angle φp
0
120°
240°
360°
1.5
1
0.5
4
3
2
10
8
6
b = 0 a.u.
b = 1 a.u.
b = 10 a.u.
b = 100 a.u.
plane wave

Second, in order to understand how the electron emission patterns change if one **departs from the paraxial approximation**, calculations have been performed for the same photon energy and helicity as before but for three different values of the parameter $s = \varkappa/k_z$: $s = 0.01$, $s = 0.1$ and $s = 1$. While the first of these values obviously corresponds to the paraxial limit, **the last one describes the general (non–paraxial) regime**.

In the next Fig. we display the angular distribution that has been evaluated for these s values as well as for the impact parameters $b = 100$, 1000 and 10000 a.u.

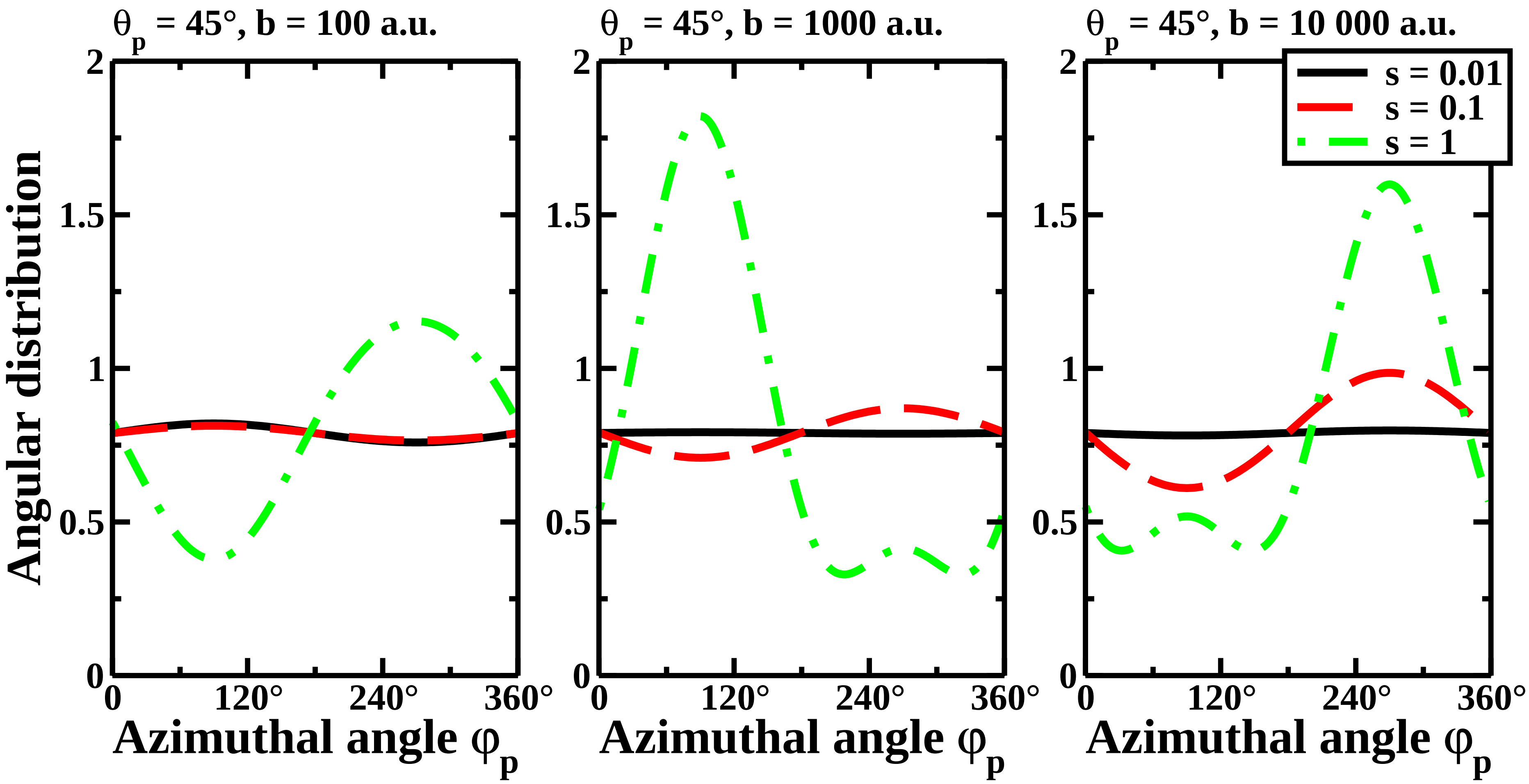

θ_p = 45°, b = 100 a.u.
θ_p = 45°, b = 1000 a.u.
θ_p = 45°, b = 10 000 a.u.
Angular distribution
0
0.5
1
1.5
2
0
120°
240°
360°
Azimuthal angle φ_p
s = 0.01
s = 0.1
s = 1

As seen from the figure, the electron emission patterns appear to be very sensitive to the variation of s. That is, while $dW(\theta_p, \varphi_p)/d\Omega$ is almost isotropic in the paraxial regime ($s = 0.01$), it shows a remarkable φ_p–dependence if the transversal component of the photon linear momentum is comparable to the longitudinal one ($s \sim 1$).

In the paper Ref. [6] we have performed a theoretical study of the cross channel to the photoionization — **the radiative recombination of the twisted electrons with low-Z bare ions**. Based on solutions of the non-relativistic Schrödinger equation for the capture into the ionic ground state, **analytical expressions** were derived for
(i) the angular distribution and
(ii) the Stokes parameters of the emitted photons.
Depending on the particular setup of the recombination experiment, these (angular and polarization) properties appear to be sensitive to the kinematic parameters such as the ratio $\varkappa/p_z$ of transverse to longitudinal momentum as well as to the "twistedness" of the incident electron beam.

6. Scattering of the twisted electrons on atoms in the Born approximation

In the paper Ref. [7] G.L. Kotkin, V.G. Serbo, A. Surzhykov (which is still in preparation) we discuss the elastic scattering of wave packets on the potential field in the situation when sizes of initial packet may be compared with the typical radius of field action.

To approach this goal, we **derive a simple and convenient expression for the number of events which generalizes the well-known Born approximation for the case when the initial beam is a wave packet, but not a plane wave**.

Certainly, the total as well as the differential number of events depends on the impact parameter $\mathbf{b}$ between the potential centre and the packet axis. We also consider **the case when a wave packet is scattered on randomly distributed potential centres**. From the experimental point of view, this case is the simplest one. For such a set-up, we obtain the expression for **the cross section averaged over impact parameters** which has a simple and transparent form. Using the obtained equations, we consider in detail four models, including

scattering of **the Gaussian wave packet** on the Gaussian potential and on the hydrogen atom;

scattering of **the twisted particle packet** on the Gaussian potential and on **the hydrogen atom**.

Certainly, models with the Gaussian wave packet can be considered as the reference ones for the more interesting models with the twisted electrons. However, the former models have an advantage of simplicity. So, first we noticed some new features in scattering of the twisted electrons in these simpler models. Then we studied them in the more realistic models. The goal of our study was to answer the following principal questions:

(i) How the averaged cross sections depends on properties of the initial wave packet?

(ii) Whether the number of events for processes with the twisted particles is considerable smaller as compare with the standard case?

(iii) How the angular distribution of final electrons depends on impact parameters $\mathbf{b}$ between the potential centre and the packet axis?

Let us point out a few nontrivial features which were revealed in this study:

1) If the initial electron is in the twisted state with **a defined quantum number m**, **the averaged cross section does not depend on m**, but rather on the conical angle of the initial packet. Moreover, the total averaged cross section is of the same order of magnitude as the standard cross section. However, if the initial electron is described by a coherent superposition of twisted states with **different quantum numbers m_1 and m_2**, **the differential as well as the total averaged cross sections do depend** on the difference $m_2 - m_1$.

2) In scattering of the twisted electrons we find that an angular distribution for **a central collision (at $b = 0$)** has **a deep in the region of small scattering polar angles** θ which **disappears with the growth of** b.

3) **Azimuthal distribution in scattering of the twisted electrons exhibits a lot of unusual features**, especially for large m. **It may be the source of additional information for scattering of the twisted electrons on more complicated and anisotropic atomic structures**.

7. CONCLUSION

The main goal of my talk was to demonstrate
that the twisted photons and electrons
may really be used as
a new tool for investigations in atomic and nuclear physics

Thus, twisted particles give us
a new degree of freedom

ORBITAL ANGULAR MOMENTUM

and will provide additional details about

the fundamental light-matter and

electron-matter interactions

THANK YOU FOR YOUR ATTENTION!